ELECTRODE SURFACE EFFECTS ON UNIPOLAR CHARGE INJECTION IN COOLED LIQUID DIELECTRIC MIXTURES

by
V. H. Gehman, Jr., D. B. Fenneman, and R. J. Gripshover
Naval Surface Weapons Center
Dahlgren, Va. 22448

SUMMARY

Previous investigations at NSWC, Dahlgren Laboratory, have established that anomalous voltage decay curves are observed for capacitors filled with cooled ethylene glycol-water dielectric mixtures. A unipolar charge injection model developed in conjunction with M. Zahn, et al, at MIT correctly predicted experimental waveforms and yielded information on the quantity of charge injection and the mobility of the transported species. Experiments are described demonstrating the effects of surface materials on the charge injection phenomenon, specifically electropolished, passivated stainless steel vs. untreated 304 stainless steel and cuprous oxide coatings vs. electrolytic copper. Analysis of the electrode surface effect is accomplished with the assistance of a computer model of the charge injection process that uses a hill climber routine to adjust physical parameters until the model matches the experimental behavior of the voltage decay curve.

INTRODUCTION

The use of water as an intermediate energy storage medium in pulsed power devices stems from its favorable physical and electrical properties: high dielectric constant, self-repairability, low cost, ease of purification, ease of handling and its inherent lack of health or safety problems. Previous work at NSWC has demonstrated that standard purification systems,[1] use of deaeration techniques and bead blasting as a surface preparation yield better and less scattered breakdown results than were previously thought practical.[2,3] As it became apparent that longer charging times would ease the requirements on the rest of the pulsed power system,[4] the relationship between purity and temperature with intrinsic time constant came under increased scrutiny. Subsequent research at NSWC demonstrated the increased time constant possible from cooled, highly purified water (approximately 670 μs), and from subzero mixtures of ethylene glycol and water (approximately 67 ms for 60 w/o glycol mixtures at -30°C).[5]

Unfortunately, as these high time constant mixtures were being studied an anomalous decay of voltage was observed that was far faster than the normal exponential decay of a dielectric filled capacitor. Upon further study the anomalous voltage waveforms were found to match the theoretical predictions of a unipolar charge injection model developed by Fenneman with M. Zahn, et al, of MIT.[6] The charge injection theory will be briefly discussed in the next section. It should be emphasized that the suppression of charge injection is desired as it would lead to longer effective time constants and would be more likely to allow charging of pulse forming lines with rotating machinery.

CHARGE INJECTION[6]

The anomalous decay of voltage in subzero glycol/water filled capacitors was found to be consistent with a unipolar charge injection model, as noted above. Because charge injection introduces a spatial dependence to the electric field, the equation describing the physical behavior of the capacitor system becomes a partial differential equation of the form:

$$\frac{\partial \tilde{E}}{\partial \tilde{t}} + \frac{\tilde{E}}{\tilde{\tau}} + \tilde{E}\,\frac{\partial \tilde{E}}{\partial \tilde{x}} = \tilde{J}(\tilde{t}) = 0 \qquad (1)$$

Where $\tilde{J}(\tilde{t}) = 0$ because the experimental circuit has a high voltage diode in place which effectively creates an open circuit with the only path left for the charge on the capacitor to ground is via decay. All variables are made unitless by normalizing all quantities with respect to the electrode spacing 'ℓ', the initial voltage 'V_o' and the nominal charge injection transfer time, '$\ell^2/(\mu V_o)$':

$$\tilde{\tau} = \frac{\epsilon}{\sigma}\Big/\left(\frac{\ell^2}{\mu V_o}\right),\ \tilde{t} = t\Big/\left(\frac{\ell^2}{\mu V_o}\right),\ \tilde{x} = x/\ell,\ \tilde{V} = V/V_o$$

$$\tilde{E} = (E/(V_o/\ell)),\ \tilde{q} = q\Big/\left(\frac{\epsilon V_o}{\ell^2}\right),\ \tilde{A} = A\ell/\epsilon \qquad (2)$$

The method of characteristics allows equation (1) to be converted into an ordinary differential equation by 'jumping' into the frame of reference of the moving charges, that is, to allow:

$$\frac{d\tilde{x}}{d\tilde{t}} = \tilde{E} \qquad (3)$$

The only remaining task before solving the differential equation is to define the boundary condition at the injecting electrode. Zahn and Fenneman, et al, chose the simplest boundary condition that was logically reasonable, namely the injected charge is equal to a constant times the instantaneous electric field at the injecting electrode, and found it worked quite well in matching experimental results. In normalized units this condition is:

$$\tilde{q}_o(\tilde{x} = 0, \tilde{t}) = \tilde{A}\,\tilde{E}_o(\tilde{x} = 0, \tilde{t}) \qquad (4)$$

Report Documentation Page

Form Approved
OMB No. 0704-0188

1. REPORT DATE	2. REPORT TYPE	3. DATES COVERED
JUN 1983	**N/A**	**-**

4. TITLE AND SUBTITLE	5a. CONTRACT NUMBER
Electrode Surface Effects On Unipolar Charge Injection In Cooled Liquid Dielectric Mixtures	5b. GRANT NUMBER
	5c. PROGRAM ELEMENT NUMBER
6. AUTHOR(S)	5d. PROJECT NUMBER
	5e. TASK NUMBER
	5f. WORK UNIT NUMBER
7. PERFORMING ORGANIZATION NAME(S) AND ADDRESS(ES) **Naval Surface Weapons Center Dahlgren, Va. 22448**	8. PERFORMING ORGANIZATION REPORT NUMBER
9. SPONSORING/MONITORING AGENCY NAME(S) AND ADDRESS(ES)	10. SPONSOR/MONITOR'S ACRONYM(S)
	11. SPONSOR/MONITOR'S REPORT NUMBER(S)

12. DISTRIBUTION/AVAILABILITY STATEMENT
Approved for public release, distribution unlimited

13. SUPPLEMENTARY NOTES
See also ADM002371. 2013 IEEE Pulsed Power Conference, Digest of Technical Papers 1976-2013, and Abstracts of the 2013 IEEE International Conference on Plasma Science. Held in San Francisco, CA on 16-21 June 2013. U.S. Government or Federal Purpose Rights License.

14. ABSTRACT

15. SUBJECT TERMS

16. SECURITY CLASSIFICATION OF:			17. LIMITATION OF ABSTRACT	18. NUMBER OF PAGES	19a. NAME OF RESPONSIBLE PERSON
a. REPORT	b. ABSTRACT	c. THIS PAGE			
unclassified	**unclassified**	**unclassified**	**SAR**	**7**	

The solution to (1) is in two parts: one case for those times less than the charge transport time, $\tilde{t}_d$, where the electric field integration must be carried out in two separate integrals and another case for times greater than the charge transport time. It can be shown that the actual charge transport time, $\tilde{t}_d$, is:

$$\tilde{t}_d = \tilde{\tau}\, \ell n\left(\frac{\tilde{\tau}}{\tilde{\tau} - 1}\right) \tag{5}$$

While the solution for $\tilde{V}(\tilde{t})$ is:

$$V(t) = \begin{cases} e^{-\tilde{t}/\tilde{\tau}}\left\{1-\frac{\tilde{\tau}}{2}\left[\frac{\tilde{A}\tilde{\tau}(1-e^{-\tilde{t}/\tilde{\tau}})^2}{1+\tilde{A}\tilde{\tau}(1-e^{-\tilde{t}/\tilde{\tau}})}\right]\right\}, & 0 \leq t \leq t_d \\ e^{-\tilde{t}/\tilde{\tau}}\ (\tilde{A}+2)/(2[1+\tilde{A}\tilde{\tau}(1-e^{-\tilde{t}/\tilde{\tau}})[), & \tilde{t} > \tilde{t}_d \end{cases} \tag{6}$$

Note that the two parameters unknown in (6) are $\tilde{A}$ and $\tilde{\tau}$, which contain information about the quantity of injected charge and the mobility of the injected species, respectively. It is these parameters that are fitted in the least squares program described later.

ELECTRODE SURFACES

The baseline electrode surface treatment for all materials was bead blasting with 125 μm glass beads (Zero-Blast-N-Peen, size 801, MIL-G-9954A). This surface had been found to give reproducable results in previous studies at NSWC and was easily applied to metal surfaces. The specific materials studied for this paper were:

(1) 304 stainless steel
(2) 7075 aluminum alloy
(3) Electrolytic, tough pitch copper
(4) 70-30 brass

The electrodes were 4" diameter planar electrodes with rounded edges and circular cross section, except for the copper electrodes that were heat treated to form cuprous oxide surface films – these were similar in shape but only 2.5" in diameter.

Alloy 304 stainless steel was a composition of approximately 18 w/o chromium, 8 w/o nickel with a maximum carbon content of 0.8 w/o. The surface treatment chosen for comparison to bead blasting was a combination of electropolishing and passivation. The electropolishing was intended to remove minute sharp edges and further planarize the electrode contour. Passivation was accomplished in a heated solution (110°F) of nitric acid and potassium dichromate. Both treatments were performed by a commercial metal finisher. Passivation was supposed to form a contiguous layer of chromic oxide across the surface of the steel preventing contamination of the liquid dielectric by metal ions. It was expected that this process would reduce the amount of charge injection, the effect on breakdown strength could not be estimated.

Similarly, the anodizing process was intended to produce a continuous layer of aluminum oxide on the 7075 aluminum electrode (composition nominally 5.6 w/o zinc, 2.5 w/o magnesium, 1.6 w/o copper, 0.3 w/o chromium, balance aluminum). It was expected that this too would reduce the amount of charge injection but again the effect on breakdown strength could not be estimated. The anodizing process was performed at NSWC and conformed to MIL-A-8625C. A brief outline of the step by step procedure consists of consecutive immersions in:

(1) Concentrated NaOH at 175°F for 2 minutes (8 oz./gal.)
(2) Cold water rinse for several minutes
(3) Chromic acid, M702, cold for 2 minutes (16 oz./gal.)
(4) Cold water rinse for several minutes
(5) Chromic acid (5% solution) and a product called Zero Mist for 30 minutes at 40 volts, low amps, 95°F
(6) Cold water rinse for several minutes
(7) Sodium bichromate solution (5%) for 10 minutes at 180°F
(8) Cold water rinse for several minutes
(9) Hot distilled water seal, 10 minutes at 175°F.

Cuprous oxide was chosen because it was a p-type semiconductor. It was thought that this coating would reduce the gradient of the electric field from the electrode to the dielectric and thereby improve the breakdown strength of the capacitor. The conductivity was found in other studies to be highly dependent on the processing history; our measurement of conductivity of the films grown for this experiment were not ready in time for this paper. The oxide layer was grown on the electrolytic copper electrodes by heat treatment in a special atmosphere furnace. The procedure was worked out from literature sources[7] and from Mr. C. S. Duncan of the Westinghouse Research and Development Center in Pittsburgh, Pa. An approximate step-by-step procedure:

(1) Clean copper blank, rinse in high purity methanol, air dry.
(2) Place in furnace, start argon flow.
(3) Raise temperature to 1050°C under inert argon atmosphere.
(4) At 1050°C, introduce small partial pressure of 0_2, typical anneal time - 10 minutes.
(5) Cease 0_2 flow, allow furnace to cool under argon.

As controls 2.5" diameter samples of copper were tested without coatings. Also brass and copper 4" diameter electrodes were tested for comparison, both with bead blasted surfaces. In order to determine the polarity effect for the stainless steel and the copper electrodes, mixed pairs were tested. That is, tests were done with one passivated steel and one bead blasted steel electrode, as well as, one cuprous oxide and bead blasted copper electrode. Mixed tests on the aluminum electrodes were not completed in time for publication.

HIGH VOLTAGE TESTING

An electrical block diagram for the testing apparatus is shown in Figure 1. The main components were a Marx

generator that charged the test cell via a copper sulfate charging resistor and a high voltage diode. A diagram depicting the liquid dielectric flow is shown in Figure 2. The experimental apparatus has been thoroughly explained in previous papers.[5]

On the basis of the previous work at NSWC, the dielectric liquid chosen for study was 60 w/o ethylene glycol and 40 w/o water. The temperature at which measurements were made was carefully chosen so as to keep the ratio of the nominal charge injection transport time to the low voltage intrinsic time constant very low – this meant that most of the charge transported through the liquid was injected rather than intrinsic charge, allowing electrode effects on charge injection to be clearly measured.

ANALYSIS

Quantitative analysis of voltage traces, that reflected greatly varying amounts of charge injection; see Figure 3, required a least squares fit of equation (6) to experimental voltage versus time data. To accomplish this a computer program of the hill-climber type was formulated which used the gradient of (6) with respect to the variables $\widetilde{A}$ and $\widetilde{\tau}$ to search for the best least squares approximation to the experimental data. The program could be set to terminate execution upon any or all of the following conditions:

(1) The sum of squared error increased
(2) The change in either $\widetilde{A}$ or $\widetilde{\tau}$ was smaller than a preset value
(3) A preset number of iterations was reached.

The convergence on the two parameters slowed as the routine progressed reflecting the fairly flat contour of the solution surface due mainly to the limited number of data points used in the program, as the oscilloscope information was digitized by hand from photographs. More automated means of analog to digital conversion of voltage signals would have given not only a larger number of data points but would have improved the accuracy of each data point.

Another computer routine reduced measured data from the voltage traces to produce three figures-of-merit: a normalized, effective time constant, $\widetilde{t}_{eff}$, the energy density, W, and the action density, AD. The effective time constant, $\widetilde{t}_{eff}$, was the same as defined by Martin, namely the time the voltage remained above 0.63 of the maximum voltage, except that it was normalized to uniform electrode spacings, peak voltages and low voltage intrinsic time constants. The reference electrode spacing was 1 cm, the reference peak voltage was 100 kV, and the reference time constant was 20 ms. The energy density, W, was:

$$W = \frac{1}{2} \epsilon \epsilon_o E^2 \tag{7}$$

where ϵ was the dielectric constant and ϵ_o was the permittivity (8.85×10^{-12} f/m). The action density was a figure-of-merit used previously by Fenneman and was simply the energy density multiplied by the normalized, effective time constant:

$$AD = \frac{1}{2} \epsilon \epsilon_o E^2 \widetilde{t}_{eff} \tag{8}$$

In equations (7) and (8) E was defined as the maximum voltage across the plates divided by the plate spacing. This distinction was necessary as charge injection introduced a spatial dependence in the electric field. This convention was also followed later when threshold breakdown strengths were calculated by dividing the maximum voltage before the onset of breakdown by the electrode spacing.

As action density was a relative measure of the energy stored in the capacitor and the time that energy can be held on the capacitor, it was the figure-of-merit used to rank electrode materials in the Conclusion section of this paper. This was done to emphasize the need for adequate hold-off times as well as breakdown strength for useful pulse forming lines.

RESULTS

CHARGE INJECTION

The result of the least squares program for the injected charge constant for different surface preparations of the 304 stainless steel was plotted in Figure 4 as a function of voltage across the plates. The two different surfaces examined, bead blasted and electropolished, passivated, were arranged in four combinations. The symmetric arrangements, where both electrodes were given the same surface treatments, were denoted by the data points labeled either 'BB' or 'EP'. The asymmetric arrangement of electrodes, where one was given a bead blasted surface and the other an electropolished, passivated surface, were denoted by the data points labeled 'EP(+), BB(-)' or 'EP(-), BB(+)'. The polarity symbols in parentheses indicated which electrode had been anode and which had been cathode.

Figure 4 indicated for the symmetric experiments that the bead blasted surface injected much more charge than the electropolished, passivated surface. The asymmetric cases demonstrated that when the anode was electropolished and passivated the amount of injected charge was approximately the same as the symmetric electropolished, passivated case, even though the cathode was bead blasted. Also, when the anode was bead blasted the amount of injected charge was roughly that of the symmetric bead blasted case, even though the cathode had been electropolished and passivated.

The direct conclusion from the symmetric experiments was that an electropolished, passivated steel surface inhibited charge injection far more thoroughly than a bead blasted surface. The inferred conclusion from studying the asymmetric experiments was that the charge injection was primarily unipolar, specifically positive. The experiments could not prove that the charge injection was purely unipolar, only that the predominant injecting species was positive. Zahn, et al, has demonstrated that, in fact, the stainless steel injected only positive carriers.

The computer program also computed $\widetilde{\tau}$ which when solved for the mobility of the injecting species always gave values at least as great as the low voltage values for the

hydronium ion found in the literature. This agrees with previous work done at NSWC. The range in computed $\tilde{\tau}$ is larger than expected but can be accounted for by the limitations of the computer search routine and the number of data points that can be digitized by hand from oscilliographs. Future work will address this problem.

STAINLESS STEEL

Action Density as a function of applied voltage for 304 stainless steel, both bead blasted and electropolished, passivated, was plotted in three time-sequential graphs, see Figures 5, 6 and 7. Figure 5 measurements were made in March, 1982, approximately one month after the electropolishing and passivation treatments. Note the superiority of the electropolished, passivated electrodes over bead blasted. Also, the asymmetric measurements indicated that the passivation treatment was far more critical for the anode than the cathode. A year after the surface treatments, in March 1983, the electrodes were retested and the beneficial effects of the electropolishing and passivation were found to nullified. Following reapplication of the surface treatments on March 18, 1983, the measurements were made again and the beneficial effects of electropolishing and passivation were recovered. In summary, the surface treatments were found to be very beneficial but were degraded with time; however, with reapplication, regained their former favorable characteristics.

ANODIZED ALUMINUM

The normalized, effective time constant and the Action Density for the other electrode materials as a function of applied voltage were plotted in Figures 8 and 9, respectively. Note that in Figure 8 the performance of the materials was roughly comparable at the low voltages; it was only due to the higher voltages that could be applied to the anodized aluminum that allowed a significant increase in this parameter over the other materials. The reason that higher voltages could be applied to the anodized aluminum was the breakdown threshold for anodized aluminum was found to be 20% higher than for untreated aluminum. Similarly, the Action Density was found to be roughly comparable except for anodized aluminum at the higher voltage levels. Compared to 304 stainless steel, electropolished and passivated, the Action Density for anodized aluminum was found to be significantly smaller.

Of interest is the work of Zahn, et al,[8] which demonstrated that copper was a positive charge injector, aluminum was a negative charge injector, and brass was a bipolar charge injector. As asymmetric experiments were not performed for aluminum and brass, but only for copper and steel, the polarity of the charge injection for those materials was not investigated in this study.

CUPROUS OXIDE

The normalized, effective time constant and the Action Density for the 2.5″ diameter electrodes used to study the native cuprous oxide layer were plotted in Figures 10 and 11, respectively. As in the stainless steel section, data was plotted for symmetric electrode pairs and asymmetric pairs. The symmetric pairs were denoted as either Cu, Cu - for copper electrodes or as Cu_20, Cu_20 - for cuprous oxide electrodes. When asymmetric results were plotted the chemical symbol was followed by either a plus sign (for the anode) or a minus sign (for the cathode). In Figure 10 it was noted that the cuprous oxide electrodes had a higher effective time constant than the plain copper electrodes while the asymmetric data points indicated that using a cuprous oxide electrode as the anode was more effective than using plain copper as an anode. Using Figure 11, it was concluded that cuprous oxide electrodes were better than plain copper and the asymmetric data demonstrated that using a cuprous oxide electrode as the anode was more effective than using plain copper. The deduction from the asymmetric data was the same as for stainless steel; the charge injection from copper is primarily unipolar and positive. The Action Density for cuprous oxide was still not as good as for electropolished and passivated stainless steel; however, the favorable mechanical performance of the oxide layer under breakdown was encouraging. If improved breakdown behavior can be obtained by varying the physical parameters of the oxide layer, such as thickness, conductivity, etc., the Action Density might still be greatly improved. For this reason, cuprous oxide was still considered to have the greatest potential for improvement of all the coatings.

CONCLUSIONS

(1) At this time, electropolished, passivated stainless steel is superior to all other electrode materials that have been evaluated at NSWC.

(2) Anodized aluminum is superior to plain bead blasted aluminum.

(3) Cuprous oxide is superior to copper and has the greatest potential for improvement in breakdown behavior.

ACKNOWLEDGEMENTS

This work was supported by the NSWC Independent Research Program. The authors would also like to express their appreciation to K. Chilton and L. W. Hardesty for their able assistance in the experimental measurements.

E. E. Rowe and N. L. Rupert also contributed to the project in discussions of the materials science aspects of the experiment.

REFERENCES

1. D. B. Fenneman and R. J. Gripshover, "Experiments on Electrical Breakdown in Water in the Microsecond Regime," IEEE Trans. Plasma Science, **PS-8**, September 1980, p.209.

1. D. B. Fenneman, "Water Capacitors for Pulse Power Applications," *Proceedings of Symposium on High Energy Density Capacitors and Dielectric Materials*, ed. C. W. Reed (Washington, D.C.: National Academy Press, 1981).

3. V. H. Gehman, Jr. and D. B. Fenneman, "Experiments on Water Capacitor Electrode Conditioning by Ion Bombardment," *Conference Record XIVth Pulsed Power Modulator Symposium*. IEEE 80 CH 1573-5 ED, 1980, p. 154.

4. D. B. Fenneman and R. J. Gripshover, "The Electrical Performance of Water Under Long Duration Stress," *Conference Record XIVth Pulsed Power Modulator Symposium*, IEEE 80 CH 1573-5 ED, 1980, p. 150.

5. D. B. Fenneman, "Pulsed High-Voltage Dielectric Properties of Ethylene Glycol/Water Mixtures," J. Appl. Phys., **53**(12), December 1982, p. 8961.

6. M. Zahn, S. Voldman, T. Takada, D. B. Fenneman, "Charge Injection and Transport in High Voltage Water/Glycol Capacitors," J. Appl. Phys, **54**(1), January 1983, p. 315.

7. Henisch, H. K., *Rectifying Semi-Conductor Contracts*, Oxford at the Clarendon Press, 1957.

8. M. Zahn, "Charge Injection and Transport Analysis and Measurements in Highly Purified Water," 4th IEEE Pulsed Power Conference, June 1983.

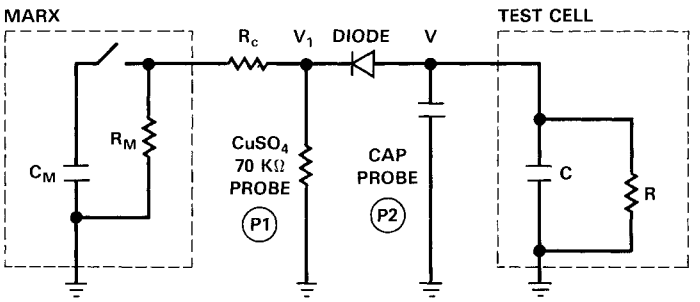

Figure 1. Electrical diagram of the liquid dielectric experimental apparatus.

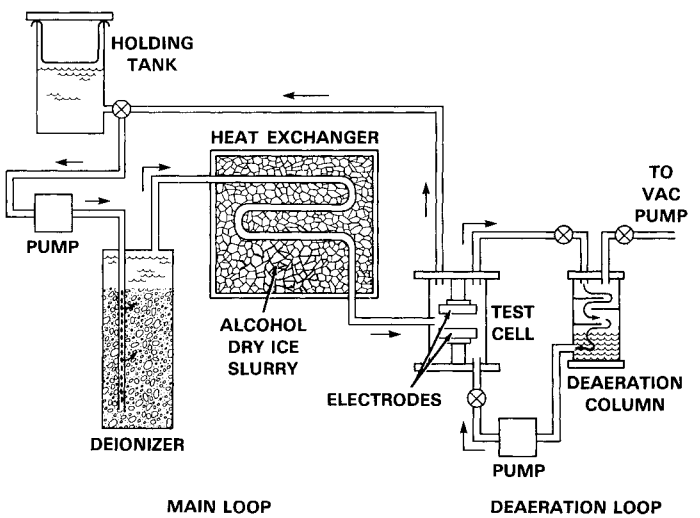

Figure 2. Liquid flow diagram for the experimental apparatus.

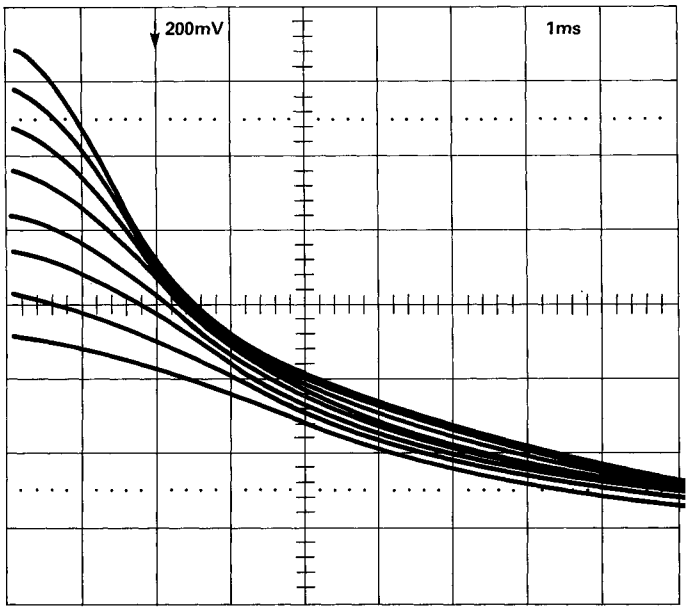

Figure 3a. Bead blasted 304 stainless steel electrodes in 60 w/o glycol, 40 w/o water liquid dielectric at ~−30°C, d=0.73 cm. Note rapid voltage drop-off due to charge injection.

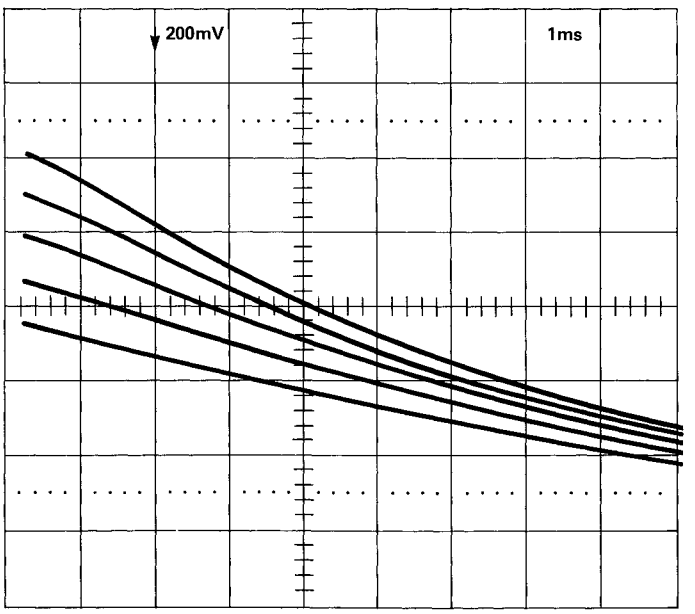

Figure 3b. Electropolished, passivated 304 stainless steel electrodes under the same experimental conditions. Note that the voltage falls off less quickly than (3a); the effect of reduced charge injection as a result of the passivated surface.

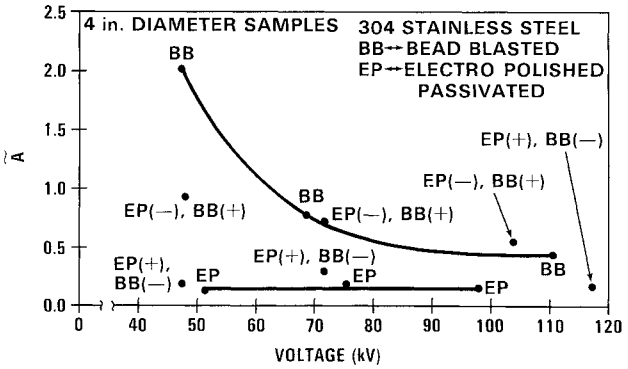

Figure 4. The normalized charge injection parameter, $\tilde{A}$, as a function of applied voltage for different coatings on 304 stainless steel.

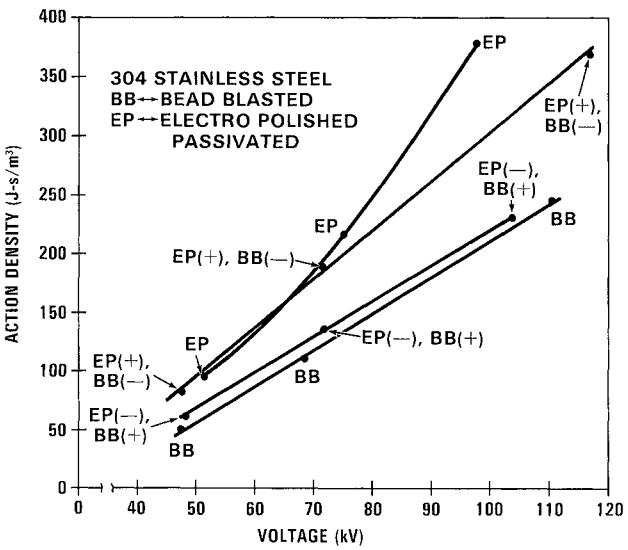

Figure 5. Action density as a function of applied voltage for 304 stainless steel electrodes. These measurements were made shortly after electropolishing and passivation treatments in March 1982.

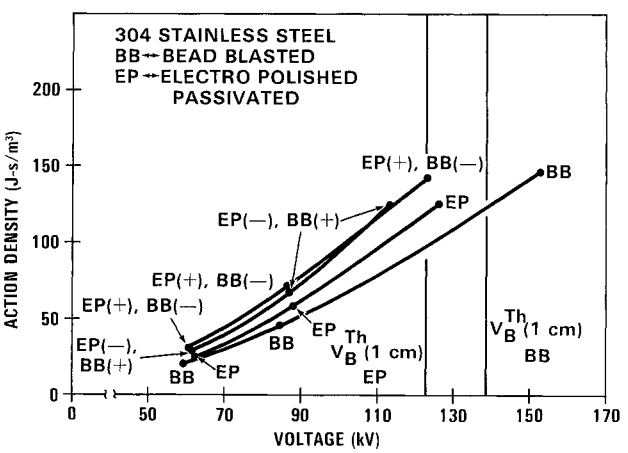

Figure 6. Action density as a function of applied voltage for 304 stainless steel. These measurements were made in early March 1983, when the passivated surface was about one year old. Note much lower values for action density as compared to Figure 5.

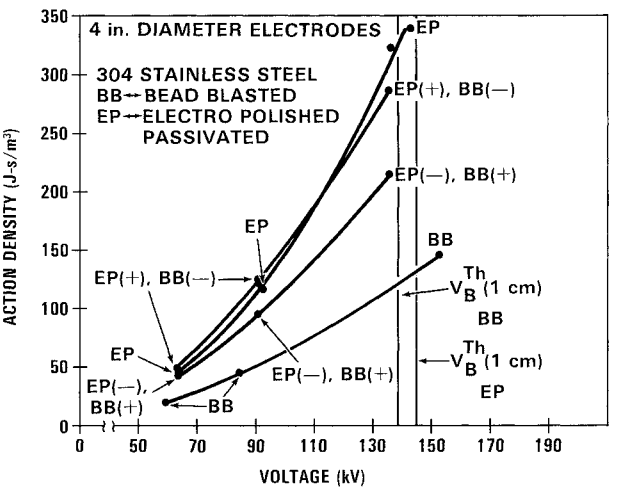

Figure 7. Action density as a function of applied voltage for 304 stainless steel. These measurements were made in late March 1983, after reapplication of the electropolishing and passivation surface treatments on 18 March 1983. Note return of action density to values comparable to Figure 5.

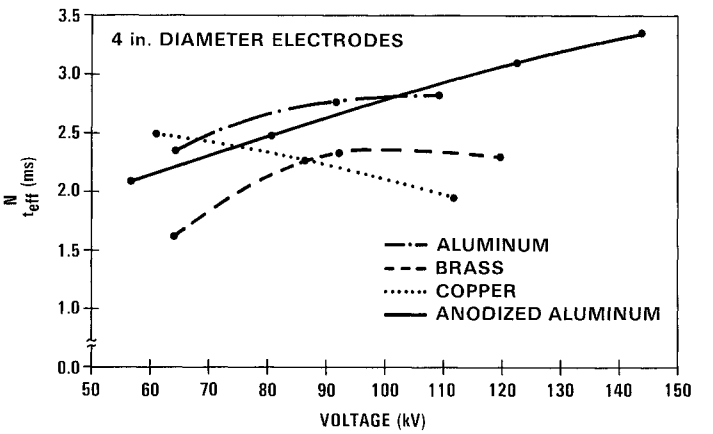

Figure 8. Normalized effective time constant as a function of applied voltage for various electrode materials.

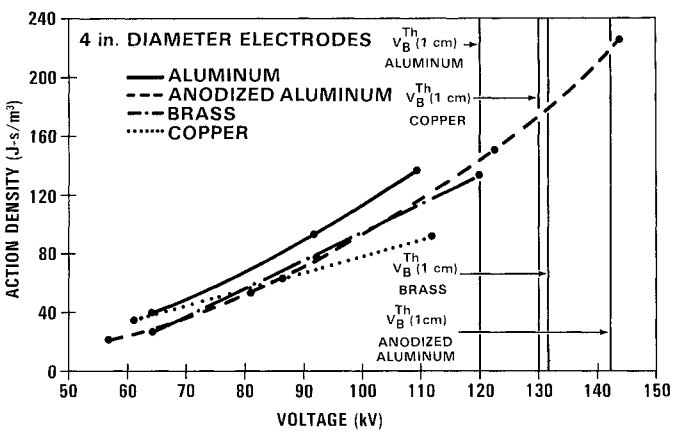

Figure 9. Action density as a function of applied voltage for various electrode materials. Note the threshold breakdown voltages (for a 1 cm gap) and the improvement of anodized aluminum over bead blasted aluminum.

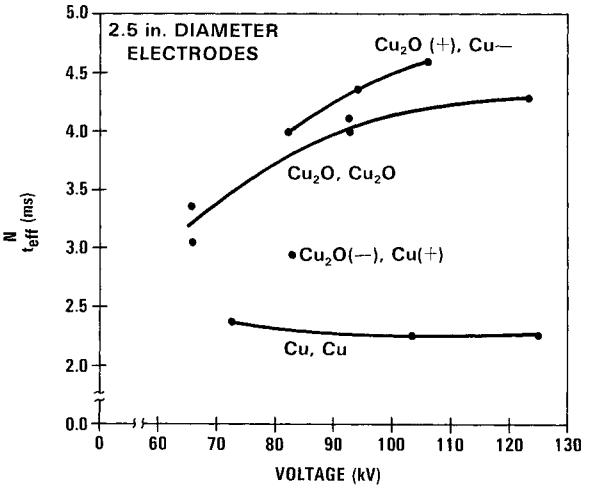

Figure 10. Normalized effective time constant as a function of applied voltage for 2.5″ diameter electrodes.

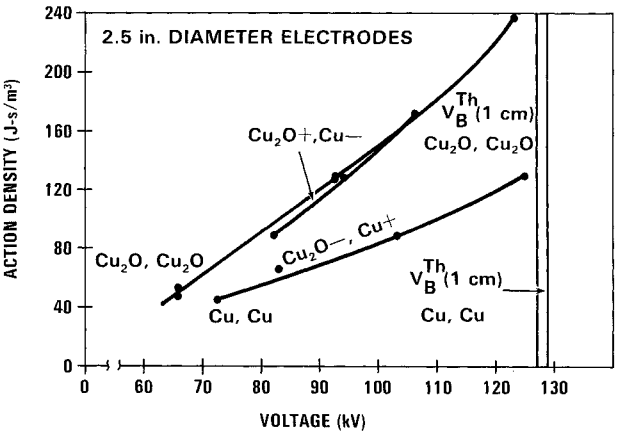

Figure 11. Action density as a function of applied voltage for 2.5″ diameter electrodes. Note the improvement in action density for cuprous oxide and that the breakdown values are roughly equivalent.